Journal of Physics: Conference Series

Comparison of Bi_2S_3 and Ta_2O_5 as alternative materials to gold in nanoparticles used as agents to increase the dose in radiotherapy

IOP Conf. Series: Journal of Physics: Conf. Series **1247** (2019) 012050 doi:10.1088/1742-6596/1247/1/012050

Comparison of Bi_2S_3 and Ta_2O_5 as alternative materials to gold in nanoparticles used as agents to increase the dose in radiotherapy

Harley Alejo-Martinez[1], Andrés C. Sevilla-Moreno[2] Alejandro Ondo-Mendéz[3,4] Jorge H. Quintero[5] and Carlos J. Páez[5]

[1]Vicerrectora de investigacin, Universidad ECCI, Bogotá, Colombia
[2]Grupo de Licenciamiento y Control, Servicio Geolgico Colombiano
[3]Grupo de investigación clínica, Escuela de Medicina y Ciencias de la Salud, Universidad del Rosario, Bogotá, Colombia
[4]Unidad de Boiquímica, Departamento de ciencias Biomédicas, Escuela de Medicina y Ciencias de la Salud, Universidad del Rosario, Bogotá, Colombia
[5]Escuela de Física, Universidad Industrial de Santander, Ciudad Universitaria , Bucaramanga 680002, Colombia

E-mail: cjpaezg@uis.edu.co

Abstract. Radiotherapy is an essential component in the treatment of all types of cancer. Radiotherapy uses ionizing radiation to destroy tumor tissue while reducing the damage to normal tissue as much as possible. In this work we study the effects of the spherical Bi_2S_3 and Ta_2O_5 nanoparticles (NPs) used as a radio-sensitization agent to increase local doses around the nanoparticle in a water medium. For low energy X-rays the dominant interaction is the photoelectric effect, which involves the absorption of a photon and the subsequent production of photoelectrons, characteristic X-rays and Auger electrons. Using a GEANT4 based simulation was determined the kinetic energy spectra of secondary electrons produced by the interaction of X-ray beam and Au, Bi_2S_3 and Ta_2O_5 NPs , after that was calculated the interaction processes, energy deposited, absorbed dose and the effective range distributions for the secondary electrons generated by the interaction of 100 million incident photons in the nanoparticles. The size of the nanoparticles was 20 nm and the energy distribution of the photons corresponds to the spectrum of a tube of x-rays with Tungsten anode and a peak voltage applied of 40 kV. This study demonstrates that Bi_2S_3 and Ta_2O_5 NPs are a viable alternative to Au NPs as a dose enhancing agent in radiotherapy.

1. Introduction

Cancer is a public health problem worldwide. Globally, each year more than 14 million new cases of cancer are diagnosed and more than 8 million die from the disease. Additionally, it is estimated that there are about 33 million people living with cancer who have been diagnosed in the last 5 years[1]. According to the World Health Organisation (WHO) more than one third of cancer cases can be prevented, and another third can be cured if it is detected early and treated.

An essential component of the treatment of all types of cancer is radiotherapy. It is prescribed for more than half of people diagnosed with cancer each year. Radiation therapy uses ionising radiations, such as X- rays, gamma rays and high energy particles, to destroy tumor tissue while

reducing the damage as much as possible to normal tissue. In recent years, the application of nanoparticles such as radio-enhancers in radiation therapy of cancer have been extensively studied, mainly because it has shown results that enhance the radiotherapeutic effects, increasing the dose given for tumors and decreasing in normal tissue[2–11].

Physically, dose enhancement is achieved by introducing nanoparticles of high atomic numbers Z in the tumor when is irradiated with low energy photons, in the range of kV. In this case, the dominant interaction is the photoelectric effect. The photoelectric effect implies the absorption of a photon by an atomic electron and the subsequent production of electrons, characteristic X-rays or auger electrons from the atom[10]. The linear attenuation coefficient, and therefore the probability of interaction, for the photoelectric effect is a function of $(Z/h\nu)^3$, where $h\nu$ is the energy of the incoming photon and Z is the atomic number of the target[11].

Agents such as iodine ($Z = 53$) and gadolinium ($Z = 64$) have demonstrated an increase in cell damage and produce localized dose enhancement at the tumor and an increase in the therapeutic effect[2–5]. Recently, the possibility of using gold nanoparticles (GNP) also has been studied for cancer radiotherapy[6–11]. Gold has also a high atomic number ($Z = 79$), compared with tissue, and the combination of GNPs and X-rays has demonstrated an increase in the effectiveness of the dose in tumor tissue, mainly associated with electrons (photoelectrons or auger electrons) produced and scattered from the gold atoms. The range of these electrons is very short and a large quantity of energy is deposited in cells containing GNP or in the proximity thereof[12].

Numerous theoretical and experimental studies have investigated the radiosensitization effect of GNPs. In a pioneering study, Herold et al[6] injected various concentrations of gold particles of 1.5-3.0 μm in mice, which were distributed in tumor tissue and exposed to kV photon beams. They showed a biologically effective dose enhancement both in vitro and in vivo. In another study, developed by Heinfeld et al[7], mice with mammary tumor received an intravenous injection of 1.9 nm diameter gold particles with a concentration of 7mg Au/g in tumors and 250 kV X-ray therapy. The results reported an 86% one-year survival compared to 20% for X-rays alone and 0% with gold alone. In this case, smaller GNPs were demonstrated to be more effective than larger gold particles in enhancing radiation therapy with X-ray.

Likewise, Monte Carlo simulations of GNPs have demonstrated physical dose enhancement for low energy photons of ^{192}Ir sources and X-rays in kilovoltage range[8, 9]. However, other studies have attributed GNP radiosensitization in the range of megavoltage energies. For example, Cho[13] evaluated the dose enhancement effect of GNPs with both kilovoltage (140 kV and ^{192}Ir) and megavoltage (4 and 6 MV) photon beams. In addition, a biological study done by Jain et al.[14] found comparable radiosensitization effect at kilovoltage and megavoltage X-ray energies. On the other hand, a study done by Chang et al. showed that in melanoma tumor-bearing mice using 13 nm diameters GNP in conjunction with a single dose of 25 Gy from a 6 MeV electron beam led to a reduction of the tumor volume than in the control groups where it was not tested.

Currently, in addition to gold nanoparticles, other materials are emerging as promising candidates in radiation oncology [15–20]. One example are materials based on bismuth and tantalum NPs. Bismuth and Tantalum have a high atomic number, Z=83 and Z = 73, respectively. This means a higher probability of interaction with incident photons and consequently higher secondary production. Tantalum pentoxide (Ta_2O_5) is a ceramic material, and biocompatible, used for orthopedic implant applications and that is being studied as a novel candidates for dose enhancement radiotherapy[16, 17]. Bismuth (III) sulfide (Ta_2O_5) nanoparticles in in vivo experiments has proven that it produces a higher inhibitory effect of the cancer cell proliferation in radiotherapy[17–19].

Many of the results can be controversial, and for this reason, one must consider that the effect of the radio-sensitization depends on factors such as energy and type of radiation, NPs

shape, size, concentration, and the location within the cell[21]. These key parameters should all be evaluated in set. The goal of the present study is to compare the increase of the local dose of promise nanomaterials with gold nanoparticles.

2. Methods

In this work was constructed a Geant4 based simulation to estimate the local absorbed dose distribution due to the interaction of an external beam and a water medium in presence of different types and concentrations of nanoparticles. In particular, to analyse the variation of local dose for nanoparticles of different materials, potentially used as radio-sensitisers, was simulated a single Bi_2S_3 or Ta_2O_5 nanoparticle with spherical shape in a segmented water phantom, finally the results are compared with the corresponding using gold. Table 1 shows the input parameters of NP1 simulation and the values used for this study.

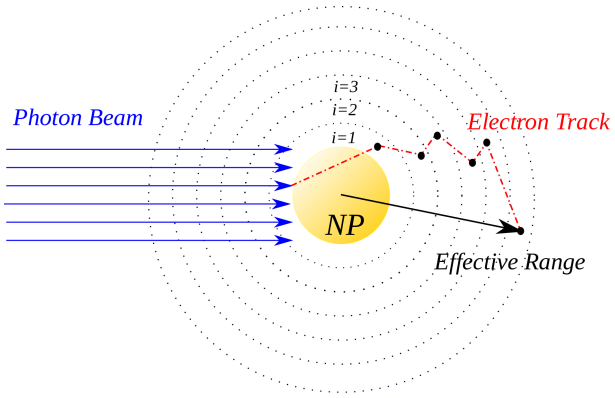

Figure 1. Schematic representation of geometry of the simulation. The effective range, the energy of the electron as it was created from the GNP and the energy deposition at each step along the electron track.

For each nanoparticle material, 100 million events were simulated. Considering the water phantom as a sensitive volume and using the stepping action class of geant4 were identified the secondary electrons produced inside the nanoparticle that arrives the water sphere and deposit energy, the corresponding event was tagged as good. Subsequently, using the tracking action class were calculated and stored the values of kinetic energy at vertex, position at vertex, final position and range. Between the start and end points of the secondary path, the deposited energy and the absorbed dose in each water shell are accumulated and stored.

3. Results and discussion

Figure 2 is a representative plot of the emission spectrum of the secondary electrons produced by the interaction of the x-ray beam and the Au, Bi_2S_3 and Ta_2O_5 NPs. The vertical axes represent the fraction of secondary electrons with a specific energy. From the interaction of the X-ray with the nanoparticles, the electrons can be produced in a variety of ways. For our discussion the relevant emissions are the photoelectrons and Auger electrons. The plots are near to each other in terms of the distribution of energy and relative counts, taking into consideration that the atomic numbers for Au, Bi and Ta are very close, $Z_Au = 79$, $Z_{Bi} = 83$ and $Z_{Ta} = 73$, and therefore, the electronic configuration and their mass attenuation coefficient in the keV energy range are very similar.

Figure 3 shows a plot of the track length or path length (left) and of the effective range (right) of secondary electrons produced from Au, Bi_2S_3 and Ta_2O_5 NPs. The vertical axis represents

Table 1. NP1 simulation parameters and selected values according to Figure 1.

Model Description	Parameter	Value
Geometry single spherical nano-particle with fixed diameter located in the center of a water phantom	NP diameter	20 nm
	NP material	Au, Bi_2S_3 and Ta_2O_5
	NP covering	none
	Phantom diameter	300nm, 10 um
	Phantom Shell thickness	3nm, 0.1 um
	Phantom material	Water
External beam Tungsten target X-Ray tube with circular cross section	particles	Photons
	Beam diameter	20 nm
	Filter object	None
	Peak tube	40 kV
	Relative voltage ripple	0 kV
Physics	Geant4 Physics List	Emstandard opt0
	Atomic Deexitation Process	Fluo, Auger, AugerCascade

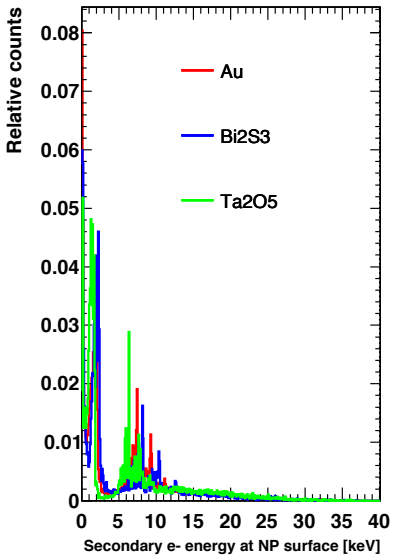

Figure 2. (a)Secondary electron emission spectrum for 20 nm nanoparticles irradiated with a 40 kVp beam for different types of nanoparticles. (b) Mass attenuation coefficient as a function of energy for (blue) gold, (red) bismuth and (green) tantalum. Theoretical mass attenuation data were obtained using published NIST mass attenuation plots.

the fraction of electrons that has finished its travel (log scale) at the distance indicated by the horizontal axis. Track length is defined as the total distance than an electron travels from the starting position at the moment of its creation to its ending position. Effective range is the displacement from the center of the nanoparticle to the ending position of the electron.

The maximum effective range of secondary electrons for the three types of NPs is at a distance greater than 10 m, which is consistent with other simulations for gold nanoparticles with energies close to 40 keV[11]. Given that the vertical axis of the graphs in figure 3 are on a logarithmic scale, it is worth noting that the higher percentage of secondary electrons have a very short effective range, therefore, in a cellular medium the effectiveness of the therapy will depend on whether the NPs are internalized into cell.

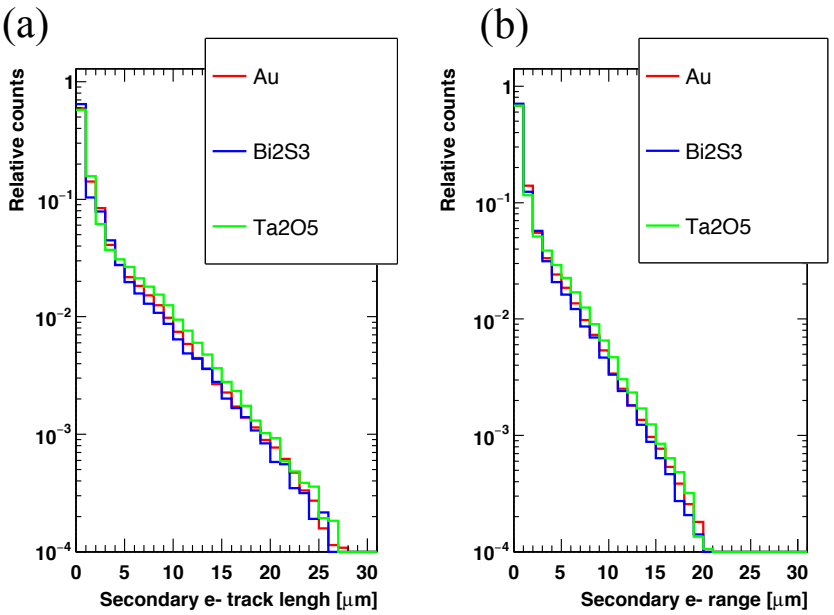

Figure 3. (a)Track length and (b) effective range of the secondary electrons emitted from different types of nanoparticles for an X-ray beam of 40 kVp.

Of all the primary photons that impact the nanoparticle we define it as a good event that the photon which leads the production of secondary electrons that escape from the nanoparticle. For each good event in the nanoparticle a certain number of secondary electrons are produced. These include the production of photoelectrons, Compton electrons and Auger cascade which consists of low-energy electrons. Table 2 shows the mean number of secondary electrons produced per good event in each NP. The standard deviation reflects the wide distribution. In relation to the greater mean number of electrons generated per good event, the order is Bi_2S_3, Ta_2O_5 and Au, respectively.

Table 2. Mean number of secondary electrons and the standard deviation of the distribution produced by ionizing event for each nanoparticle.

NP	Mean	Standard deviation
Au	3.33	1.56
Bi2S3	3.52	1.62
Ta2O5	3.37	1.29

Figure 3(a) shows a plot of the energy deposited per secondary electrons and figure 3(b) shows absorbed dose in water around the NPs as a function of distance from the center of the

NP, for a poly-energetic X-ray beam of 40 kVp and the different types of NPs. The vertical axis represents the energy deposited and the absorbed dose per good event, respectively. The absorbed dose is calculated by dividing the energy deposited to the water volume by the mass of the water shell. In both cases, it is visualised that by good event there is a greater energy delivery, and therefore, also an absorbed dose in water, for both tantalum pentoxide and bismuth (III) sulphide compared with gold.

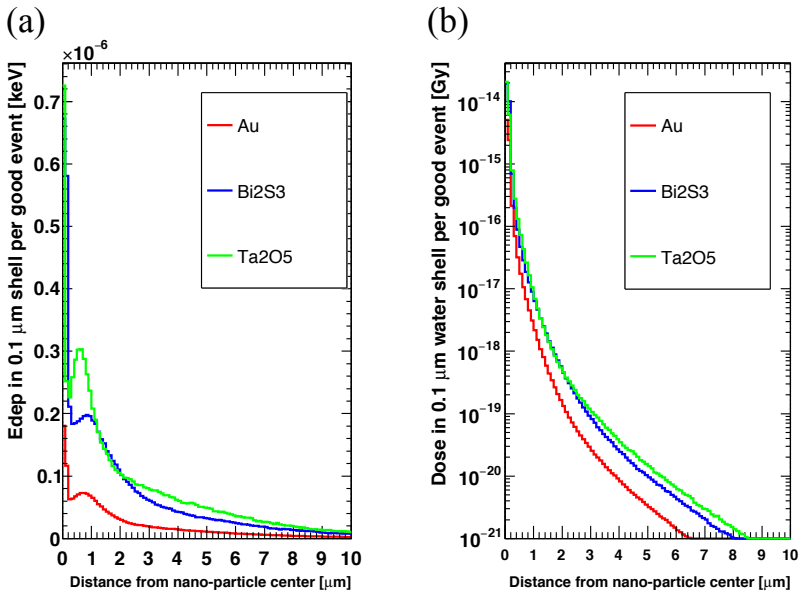

Figure 4. (a)Energy deposited and (b) absorbed dose in water per good event as a function of the radial distance from the center of the nanoparticle.

Figure 5 shows the number of good events per photon incident for the three types of nanoparticles. For Au, the value is $1.16x10^{-3}$, for Bi_2S_3, $3.64x10^{-4}$ and for Ta_2O_5, $3.3x10^{-4}$. This means that with the gold nanoparticles, good events are produced three times more often compared to the other two types of nanoparticles analysed.

Finally, in figure 5(b) we have the plot of the energy deposited and in figure 5(c) the absorbed dose in water around the NPs for each photon incident. This plot combines the results shown in figure 4 and figure 5(a). From the plot it is observed that the dose and the shape of the dose profile for the three types of nanoparticles are very similar. If we calculate the total absorbed dose for each incident photon, Bi2S3 NPs provide the maximum dose, of 1.1110^{-17} Gy, while Ta2O5 NPs have a slightly higher dose than Au NPs, of 9.3510^{-18} while Gy has 9.1610^{-18}, respectively. Bismuth (III) sulphide and tantalum pentoxide nano-materials turn out to be favorable for radiotherapeutic applications, considering that the quantitative results show to be very similar to the gold that is the baseline.

4. Conclusion

In this work we used a Monte Carlo simulation to obtain an estimation of the increases of doses of bismuth (III) sulphide and tantalum pentoxide nanoparticles compared with gold nanoparticles. Energy deposited and absorbed dose from secondary electrons, generated by X-ray irradiation of nanoparticles have been considered. Maximum dose for each incident photon from the 40 kVp X-ray source were obtained in the case of bismuth (III) sulphide nanoparticle, followed by tantalum pentoxide. The numerical results of this study complement another type of experimental studies

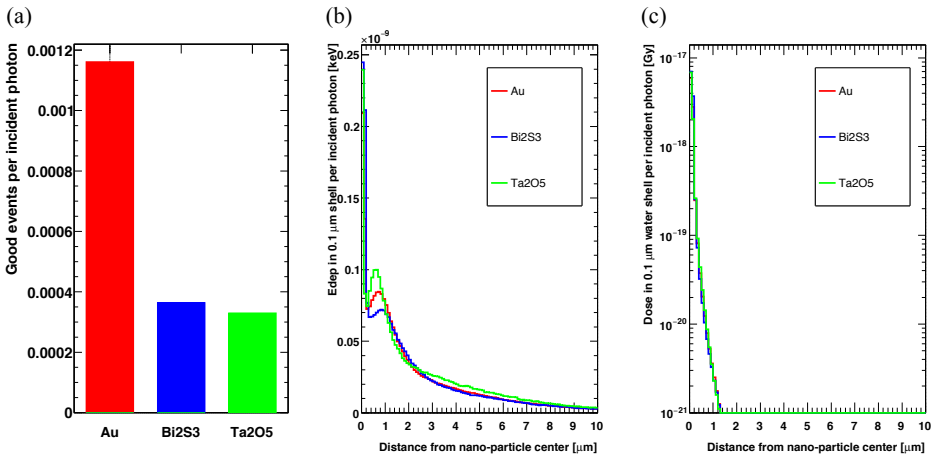

Figure 5. (a) Good events per incident photon for the three types of nanoparticles. (b) Energy deposited and (b) absorbed dose in water per incident photon as a function of the distance from the center of the nanoparticle.

that show the potential for these types of materials, in addition to the radio sensitisation effect to enhance radiation dose with respect to gold, has advantages in terms of its biocompatibility properties and costs.

References

[1] agency for research on cancer I 2012 Estimated cancer incidence, mortality and prevalence worldwide in 2012. world health organization. Website accessed on 14 July, 2014
[2] Mesa A V, Norman A, Solberg T D, Demarco J J and Smathers J B 1999 *Physics in Medicine & Biology* **44** 1955
[3] Robar J L, Riccio S A and Martin M A 2002 *Physics in Medicine & Biology* **47** 2433
[4] Dawson P, Penhaligon M, Smith E and Saunders J 1987 *The British Journal of Radiology* **60** 201–203 pMID: 3815019
[5] Matsudaira H, Ueno A M and Furuno I 1980 *Radiation Research* **84** 144–148
[6] Herold D M, Das I J, Stobbe C C, Iyer R V and Chapman J D 2000 *International Journal of Radiation Biology* **76** 1357–1364
[7] Hainfeld J F, Slatkin D N and Smilowitz H M 2004 *Physics in Medicine & Biology* **49** N309
[8] SX Z, J G, TA B, Z W, MR S and RA D 2009 *Biomed Microdevices* **11** 925
[9] Jones B L, Krishnan S and Cho S H 2010 *Medical Physics* **37** 3809–3816
[10] LEO W R 1994 *Techniques for nuclear and particle physics experiments: a how-to approach* (Springer)
[11] Johns H E; Cunningham J R 1983 *The Physics of Radiology 4th* (Springfield)
[12] Leung M K K, L J C, B C, Chithrani D, G M J, Oms L B and Jaffray D A 2011 *Medical Physics* **38** 624
[13] Cho S H 2005 *Physics in Medicine & Biology* **50** N163
[14] Jain S, Hirst D G and O'Sullivan J M 2012 *The British journal of radiology* **85** 101–113
[15] Hossain M and Su M 2012 *The journal of physical chemistry. C, Nanomaterials and interfaces* **116** 23047–23052
[16] McKinnon S, Engels E, Tehei M, Konstantinov K, Corde S, Oktaria S, Incerti S, Lerch M, Rosenfeld A and Guatelli S 2016 *Physica Medica* **32** 1216–1224
[17] Brown R, Tehei M, Oktaria S, Briggs A, Stewart C, Konstantinov K, Rosenfeld A, Corde S and Lerch M 2014 *Particle & Particle Systems Characterization* **31** 500–505
[18] Ma M, Huang Y, Chen H, Jia X, Wang S, Wang Z and Shi J 2015 *Biomaterials* **37** 447–55
[19] M A, M G, T P, A B and Lu 2015 *NanoWorld J* **3** 99–104
[20] Sherck N J and Won Y Y 2017 *Medical Physics* **44** 6583–6588
[21] Brun E, Sanche L and Sicard-Roselli C 2009 *Colloids and surfaces. B, Biointerfaces* **72** **1** 128–34